Biochimica et Biophysica Acta 1848 (2015) 3166–3174

Contents lists available at ScienceDirect

Biochimica et Biophysica Acta

journal homepage: www.elsevier.com/locate/bbamem

Functional characterization of a fatty acid double-bond hydratase from *Lactobacillus plantarum* and its interaction with biosynthetic membranes

Joana Ortega-Anaya, Alejandra Hernández-Santoyo *

Departamento de Química de Biomacromoléculas, Instituto de Química, Universidad Nacional Autónoma de México, Circuito Exterior, Ciudad Universitaria, Coyoacán, DF C.P. 04510, Mexico

ARTICLE INFO

Article history:
Received 26 May 2015
Received in revised form 18 August 2015
Accepted 14 September 2015
Available online 21 September 2015

Keywords:
Linoleic acid
10-Hydroxy-12-cis-octadecenoic acid
Lactobacillus plantarum
Fatty acid hydratase
Flavoenzyme
Fluorescent proteoliposomes

ABSTRACT

Hydrogenation of linoleic acid and other polyunsaturated fatty acids is a detoxification mechanism that is present in the *Lactobacillus* genus of lactic bacteria. The first stage in this multi-step process is hydration of the substrate with formation of 10-hydroxy-9-*cis*-octadecenoic acid due to fatty-acid hydratase activity that has been detected only in the membrane-associated cell fraction; however, its interaction with the cell membrane is unknown. To provide information in this respect we characterized the homotrimeric 64.7 kDa-native protein from *Lactobacillus plantarum*; afterwards, it was reconstituted in proteoliposomes and analyzed by confocal fluorescence microscopy. The results showed that hydratase is an extrinsic-membrane protein and hence, the enzymatic reaction occurs at the periphery of the cell. This location may be advantageous in the detoxifying process since the toxic linoleic acid molecule can be bound to hydratase and converted to non-toxic 10-hydroxy-9-*cis*-octadecenoic acid before it reaches cell membrane. Additionally, we propose that the interaction with membrane periphery occurs through electrostatic contacts. Finally, the structural model of *L. plantarum* hydratase was constructed based on the amino acid sequence and hence, the putative binding sites with linoleic acid were identified: site 1, located in an external hydrophobic pocket at the C-terminus of the protein and site 2, located at the core and in contact with a FAD molecule. Interestingly, it was found that the linoleic acid molecule arranges around a methionine residue in both sites (Met154 and Met81, respectively) that acts as a rigid pole, thus playing a key role in binding unsaturated fatty acids.

1. Introduction

Linoleic acid (LA; 18:2 $^{\Delta 9Z,12Z}$), along with other polyunsaturated fatty acids, are toxic to many bacteria causing the inhibition of cell growth. Moreover, they may deteriorate cellular membranes and block native fatty acid biosynthesis via the inhibition of enoyl-ACP reductase [1–4]. In order to prevent this toxicity, polyunsaturated fatty acids are enzymatically hydrogenated by a mechanism called biohydrogenation which is the complete reduction of double bonds on the carbon chain, producing non-toxic saturated fatty acids as the final product [5]. This process involves various steps and has been best described for LA and oleic acid (OA; 18:1 $^{\Delta 9Z}$) which are converted to non-toxic saturated stearic acid (SA; 18:0) by rumen microbiota [5–8].

Lactic bacteria belonging to *Lactobacillus* genus, such as *Lactobacillus plantarum*, are also known to biohydrogenate LA and other polyunsaturated fatty acids through a newly discovered and intricate metabolism consisting of multiple reactions catalyzed by multiple proteins (CLA-HY, CLA-DH, CLA-DC and CLA-ER) that generate characteristic fatty acid species (such as hydroxy fatty acids, oxo fatty acids, conjugated fatty acids and partially saturated *trans* fatty acids) as the intermediates to finally produce saturated monoenes (OA and *trans*-vaccenic acid) [9–11]. The first step in biohyrogenation occurring in *L. plantarum* is hydration of the Δ9Z double bond of LA which is mediated by a 64 kDa membrane-associated protein producing 10-hydroxy-12-*cis*-octadecenoic acid (10-HOE; 18:1 $^{\Delta 12Z}$) as the only product (Fig. 1) [9,12].

Once 10-HOE is produced, it can suffer various reactions (oxidation of hydroxyl group, reduction of oxo group, dehydration and isomerization) catalyzed by the linoleate isomerase complex (CLA-DH, CLA-DC, CLA-DH and CLA-ER), which has been partially characterized recently, to finally produce monoenoic acids and conjugated linoleic acid isomers (CLA; 18:2 $^{\Delta xX,yY}$) [9–11,13]. Bioactive conjugated isomer 9-*cis*-11-*trans*-octadecadienoic acid (9-*cis*-11-*trans* CLA; 18:2 $^{\Delta 9Z,11E}$) produced by the multi-component enzymatic system in *L. plantarum* has been associated with a variety of health promoting effects [14,15] such as anti-obesity and antiadipogenic activities [16], anticarcinogenic activity [17] and modulation of immune functions [18].

There are fatty acid isomerases which concertedly convert LA into a bioactive isomer of CLA (i.e. without formation of hydroxyenoic fatty

Abbreviations: 10-HOE, 10-hydroxy-12-*cis*-octadecenoic acid; CLA, conjugated linoleic acid; DMPC, 1,2-dimyristoyl-sn-glycero-3-phosphocholine; FAD, flavin-adenine dinucleotide; LA, linoleic acid; LAH, *Lactobacillus acidophilus* hydratase; LPH, *Lactobacillus plantarum* hydratase; MCRA, myosin-cross-reactive antigen; OTGP, octyl-β-D-glucopyranoside; POPC, 1-palmitoyl-2-oleoyl-*sn*-glycero-3-phosphocholine.

* Corresponding author.
E-mail addresses: joanna@comunidad.unam.mx (J. Ortega-Anaya), hersan@unam.mx (A. Hernández-Santoyo).

http://dx.doi.org/10.1016/j.bbamem.2015.09.014
0005-2736/

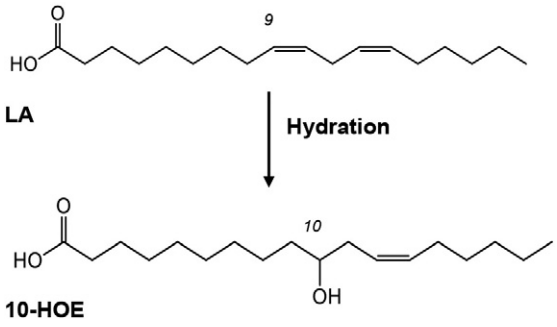

Fig. 1. Hydration of LA in *Lactobacillus plantarum*.

acids); however, to date, only three bacterial linoleate isomerases derived from *Butyrivibrio fibrisolvens*, [19], *Clostridium sporogenes* [20] and *Propionibacterium acnes* [21] have been biochemically characterized. Out of the three proteins, only *P. acnes* isomerase (PAI) has been structurally characterized as a FAD-dependent protein that produces 10-*trans*-12-*cis*-CLA [21,22].

In recent years, some proteins belonging to the myosin-cross-reactive antigen (MCRA) family have been identified as FAD-containing hydratases that act on the Δ9Z and Δ12Z double bonds of C16 and C18 non-esterified fatty acids with the formation of 10-hydroxy and 10,13-dihydroxy fatty acids in several bacteria [12,23–26]. Hydratase form *Lactobacillus acidophilus* (LAH; PDB code: 4ia5 and 4ia6) has been the only MCRA (591 residues and 67.7 kDa) from the *Lactobacillus* genus to provide structural and mechanistic information about the hydration reaction [27]. It showed that the only product from hydration of LA was 10-HOE and that hydroxyl group added to Δ9Z comes from a water molecule located at the hydrophobic substrate channel or binding site. LAH also binds one FAD molecule through a FAD-binding motif that has a structural and stabilizing role on the protein rather than participating in the catalytic reaction and is easily lost during purification of the homodimeric hydratase [27].

In this study, we investigated the biochemical properties of native MCRA from *Lactobacillus plantarum* ATCC 8014 which has only been described as a fatty acid double-bond hydratase and a FAD-containing protein by means of sequence analysis [12]. Here, the protein is denoted as LPH (*L. plantarum* hydratase) and was isolated in its native form. Furthermore, we propose a three-dimensional arrangement of the protein and performed a molecular docking with a LA molecule in order to comprehend the binding sites of the substrate which were identified and characterized as two hydrophobic pockets with amino acid residues identical to those from the fatty acid-hydratases from *L. acidophilus* (LAH) and *Elizabethkingia meningoseptica* (EMH) and those from LA-isomerase from *Propionibacterium acnes* (PAI).

Previous reports have shown that MCRA from *L. plantarum* AKU 1009a is present in the cell membrane fraction [9], however, no further experiments have been carried out to establish the nature of this membrane association, so in order to determine the interaction of native LPH with biomimetic membranes, we reconstituted the protein in DPPC:POPC proteoliposomes which were fluorescent labeled and further characterized by confocal fluorescence microscopy. These results shed light into the putative location of the hydration reaction of LA in *L. plantarum* cells and its role in the detoxifying process from polyunsaturated fatty acids.

2. Materials and methods

2.1. Bacterial strain and growth conditions

L. plantarum CFQ-100, a subculture of *L. plantarum* ATCC 8014 strain, was purchased from the WDCM 100 Culture Collection (*World Federation for Culture Collections*) of Faculty of Chemistry, UNAM, Mexico and subsequently cultured throughout all the experiments to obtain fresh cells. The strain was grown in 20 mL of MRS broth (*CONDA Lab*, *Spain*) supplemented with 180 μg/mL of LA (99% purity, *Sigma Chemical Co*., *USA*) emulsified with 0.30% (*w*/*v*) of Tween 80 and incubated at 30 °C with shaking (120 strokes/min) for 17.5 h so the cell growth has reached the end of the log phase without reaching the stationary phase. 10 mL of this seed culture was transferred into 1000 mL of fresh MRS/LA broth and incubated under the same conditions. The cell pellet was harvested by centrifugation (10,000 ×*g*, 30 min, 4 °C) and washed with 30 mL of sterile 0.85% NaCl. The biomass yield production was between 8.5–13 g/L (wet weight).

2.2. Enzyme purification

The harvested cell pellet was suspended in lysis buffer, which consisted of 100 mM potassium phosphate buffer pH 6.5 with 50 mM NaCl, 1 mM DTT and 1 mM PMSF. The suspension was then sonicated in a Misonix 3000 sonicator (*Qsonica LLT*, *USA*) using two cycles of 45 W for 5 min each. After that, the cell debris and unbroken cells were separated with centrifugation (10,000 ×*g*, 30 min, 4 °C) and the clear supernatant was used. This crude extract was ultracentrifuged (200,000 ×*g*, 60 min, 4 °C) to obtain the membrane-associated protein fraction observed as a gel-precipitate.

The membrane precipitate was solubilized with solubilizing buffer, which contained 20 mM potassium phosphate pH 6.5 with 50 mM NaCl, 10% glycerol, 1 mM DTT and 1 mM PMSF. The extraction and solubilization of membrane proteins was achieved through the addition of increasing concentrations of octyl-β-D-glucopyranoside (OTGP, *Sigma Chemical Co*., *USA*) starting from 4 mM, followed by 6 mM and finally 9 mM where the critical micelle concentration (CMC) was reached. This gradual procedure is pivotal for achieving the extraction of membrane proteins while maintaining their stability in solution [28].

Solubilized membrane proteins were first fractioned by selective precipitation with 1.5 M $(NH_4)_2SO_4$ (*High Purity Reactivos Analíticos*, *Mexico*) and LPH was found only in the supernatant fraction which was further dialyzed (20×) using a membrane with a molecular weight cutoff between 12 and 14 kDa against solubilizing buffer supplemented with 9 mM OTGP and 0.1 mM FAD (*Sigma Chemical Co*., *USA*). Afterwards, this fraction was subjected to gel filtration chromatography in a Bio SEC-5 column (4.6 mm × 150 mm × 5 μm, *Agilent Technologies*, *Germany*) using a HPLC system (*HP Agilent 1100 series, Agilent Technologies*, *Germany*) equilibrated with 20 mM phosphate buffer pH 6.5 containing 50 mM NaCl. Protein fractions were eluted with the same buffer at a flow rate of 1 mL/min, collected and analyzed for hydratase activity.

2.3. Hydratase activity assay

Unless otherwise stated, each hydration reaction was performed in triplicate and consisted on 5 mL of 20 mM potassium phosphate buffer pH 6.5, 100 μL of protein extract and 20 μg of LA as the substrate, emulsified with 0.25% (*w*/*v*) of Tween 80. The reaction was carried out for 24 h at 30 °C and 200 strokes/min. Two negative controls were used consisting in all the components except LA and all the components except the protein extract.

After incubation, the lipids were extracted with 4 mL of a chilled mix of hexane–ethyl acetate (70%–30%) and then subjected to two cycles of freeze–thawing, followed by centrifugation (3,500 ×*g*, 40 min, 4 °C) to break the emulsion previously formed. Afterwards, the organic phase was separated from the aqueous phase and washed with 1 mL of saturated NaCl. Finally, it was washed with 2 mL × 2 of deionized H_2O, dried overnight with anhydrous Na_2SO_4 and then filtered through Whatman 2 paper. The fatty acids in the organic phase were methylated and then analyzed by GC to determine 10-HOE production (see Section 2.4).

2.4. Analysis of fatty acids

Fatty acids in hexane–ethyl acetate, were dried using a water bath at 40 °C under non-oxidizing conditions with a stream of N_2. After that, they were methylated by incubation with 2 mL of 1% H_2SO_4 in methanol (*v*/*v*) at 35 °C for 30 min [29]. The organic phase was extracted with hexane, neutralized with 1 mL of saturated $NaHCO_3$ and washed with 2 mL × 2 of deionized H_2O, dried with anhydrous Na_2SO_4 and finally evaporated for GC analysis.

Fatty acid methyl ester derivatives (FAMEs) were separated, identified and quantified by a polar Heliflex™ Aqua Wax-DA capillary column (30 m length, 0.25 mm diameter and 0.25 m d_f) (*Alltech GmbH*, Germany) using an Agilent 6890 gas chromatographer (*Agilent Technologies*, *USA*) coupled to a FID detector at 240 °C. The injection volume was 1 μL and a programmed temperature vaporizer (PTV) was used in a split ratio of 1:60. Injection temperature was 240 °C. The temperature program was as follows: the initial oven temperature at 180 °C was held for 0.5 min and increased at 0.5 °C/min to reach 230 °C for 13 min. Hydrogen was used as the carrier gas with a constant flow rate of 1.8 mL/min.

Standard LA and previously purified 10-HOE (see Section 2.5) were used to identify the hydration products by comparison of retention times. The amount of 10-HOE produced was calculated from the integrated area of each peak, as total 10-HOE obtained in mg.

2.5. Purification of 10-HOE

Hydroxylated enoic acids derived from fatty acids, such as 10-HOE are not commercially available, so in order to identify 10-HOE as the reaction product of LPH, fatty acids produced from the hydration of LA were separated by high performance liquid chromatography [20] in a Luna 5u C18(2) preparative column (50 mm × 21.20 mm × 5μ d_f) (*Phenomenex*, *Inc*., *USA*) using a HPLC system (*Waters 1525 binary pump*, *Waters Corp*., *USA*) coupled to a photodiode-array detector (*Waters 2996*, *Waters Corp*., *USA*). The elution was performed with acetonitrile–water (60%–40%) at a flow rate of 12 mL/min. The injection volume was 200 μL and detection was set at 205 nm. Finally, 10-HOE was identified by GC–MS (*GCMate II*, *Jeol*, *USA*) with electron impact ionization source.

2.6. FAD assay

Purified native LPH (100 μL at a concentration of 0.5 mg/mL) was incubated at 4 °C for 16 h with different concentrations of FAD ranging from 0 to 0.1 mM. After that, hydratase activity was measured in triplicates in order to calculate the amount of bound FAD for optimal activity.

2.7. Effect of reaction conditions on hydratase activity and stability

Using fluorescence-based thermal shift assays of native LPH, we studied the effects of various pH values and additives on the stability of the protein [30]. Assays were performed with 10 μL of purified LPH (in 20 mM potassium phosphate buffer pH 6.5 with 50 mM NaCl, 10% glycerol, 9 mM OTGP and 1 mM FAD) mixed with 10 μL of each condition and added with a 1:1000 dilution of SYPRO Orange dye (*Invitrogen*, *Life Technologies*, *USA*) whose $\lambda_{excitation} = 490$ nm and $\lambda_{emission} = 575$ nm [22]. Fluorescence was recorded with a RT-PCR instrument (*Life Technologies*, *USA*) while the temperature was increased in a continuous step from 25–95ºC. For the analysis of different additives we used the Additive screen HT kit with 96 different conditions (*Hampton Research Corp*., *USA*) which in general, consisted on various sets of reagents included multivalent ions, salts, dissociating agents, linkers, polyamines, chaotropes, reducing and chelating agents, polymers, carbohydrates, polyols, amphiphiles, detergents, sulfobetaines and organic solvents (volatile and non-volatile) at various concentrations. For the analysis of pH values, we used the Wizard pH buffer kit with 96 different conditions (*Rigaku Reagents Inc*., *USA*) which consisted on sets of buffering salts at different pH values including sodium lactate-HCl (pH 2.4–5.2), sodium acetate–acetic acid (pH 3.4–6.2), MES-NaOH (pH 4.6–7.4), bis/tris–HCl (pH 5.2–8.0), imidazole–HCl (pH 5.4–8.2), sodium and potassium phosphate (pH 5.8–8.6), HEPES–NaOH (pH 6.0–8.8), tris–HCl (pH 6.6–9.4), bicine–NaOH (pH 7.0–9.8), CHES–NaOH (pH 8.0–10.8), glycine–NaOH (pH 8.2–11.0) and CAPS–NaOH (pH 8.8–11.6). Final concentration of each condition tested was half of the initial value since it was diluted 1:1 with the protein.

2.8. Structural modeling of LPH and molecular docking with LA

3D-Structure of LPH was produced using Robetta Server (automated protein structure prediction service for *ab initio* and comparative modeling) [31,32]. The amino acid sequence of LPH protein was retrieved from GenBank (accession number CBY45494.1). The server used the *ab initio* method combined with the crystallographic structure of LAH (PDB code: 4ia5) chosen automatically by its 32% sequence homology. Once the structure was built, we used Coot program version 0.8 [33] to correct geometrical parameters. Finally the overall stereo chemical quality of the model was assessed using PROCHECK program [34] on the Swiss MODEL Workspace [35]. Docking studies were carried out by using the program AUTODOCK 4.0 [36]. Hydrogens and Kollman charges were assigned to the receptor and the ligands were assigned with Gasteiger charges and nonpolar hydrogens using AutoDockTools 1.5.7. Docking simulations were run using Lamarckian Genetic algorithm that is known to be the most efficient and reliable method of Auto Dock. The grid maps were calculated using AutoGrid. Initially, potential binding sites were detected, based on the blind docking in which the box was sufficiently large to cover the whole protein 90 Å × 90 Å × 90 Å centered at the center of protein, The next step was a focused docking with a smaller box (40 Å × 40 Å × 40 Å), centered on the best energy result obtained in the blind docking. For all docking parameters, standard values were used as described before, except the amount of independent docking runs performed for each docking simulation, which was set to 200. Cluster analysis was performed on the docked results using a root mean square (RMS) tolerance of 0.5 Å, and the initial coordinates of the ligand were used as the reference structure.

2.9. Reconstitution of LPH into liposomes and confocal fluorescent microscopy (CFM)

Unilamellar proteoliposomes were prepared by the extrusion method mediated by OTGP, which is based on that first outlined by Bangham et al. [37,38]. Briefly, 1-palmitoyl-2-oleoyl-*sn*-glycero-3-phosphocholine (POPC) and 1,2-dimyristoyl-sn-glycero-3-phosphocholine (DMPC) (*Sigma Chemical Co*., *USA*) at a molar ratio of 1:1 were mixed with 0.1% (molar fraction) of β-BODIPY® FL C_5-HPC (*Life Technologies*, *USA*) as the hydrophobic fluorescent probe which is a phospholipid analog. The mix was dissolved in chloroform–methanol (1:1) and then deposited as a thin film on a round flask by rotary evaporation under reduced pressure. The dry lipid film was hydrated with 20 mM potassium phosphate buffer pH 6.5 in order to obtain a suspension of multilamellar vesicles which were further extruded through polycarbonate membranes (pore size of 200 nm; *Avanti Polar Lipids*, *Inc*., *USA*) 13 times using the Mini-Extruder set (*Avanti Polar Lipids*, *Inc*., *USA*) at 25 °C to form unilamellar liposomes that were left overnight at 4 °C.

Proteoliposomes were produced by adding freshly purified LPH (0.2 mg/mL final concentration) in 20 mM potassium phosphate pH 6.5, 0.1 mM FAD, 10% glycerol, 15 mM OTGP and Rhodamine B (5 μg/mL final concentration) (*Sigma Chemical Co*., *USA*) as the hydrophilic fluorescent probe. The excess of detergent, FAD and glycerol was removed by slow dialysis against 20 mM potassium phosphate buffer pH 6.5 with a molecular weight cut-off membrane of 14 kDa.

A 5 μL aliquot of LPH proteoliposomes was placed on a glass slide (1 × 3 in approx. 1.0 cm) with a cover slip (102 × 76 mm) and sealed with nail polish. Afterwards, it was analyzed by confocal laser scanning microscopy (Leica TCS SP5 X, *Leica Microsystems*, *Germany*) [39] using a 494 nm excitation laser and an emission range of 501–543 nm for BODIPY FL C_5-HPC. A detection and 554 nm excitation laser and an emission range of 588–648 nm for Rhodamine B. All micrographs were captured with the same settings. For three-dimensional image projection of vesicles, z-scans in 0.3–0.49 μm increments were taken through the upper half of a proteoliposome. These scans were then combined and color-merged using the LAS AF lite software Version 4.3 (*Leica Microsystems*, *Germany*).

Control experiments were carried out preparing fluorescent liposomes exactly as stated before except without the addition of LPH.

3. Results

3.1. Purification of native LPH

Native LPH purification was achieved by pelleting plasmatic membranes and membrane components by ultracentrifugation as a first step. LA hydratase activity was detected only in this membrane-associated protein fraction and not on the soluble protein fraction. LPH was extracted and solubilized using neutral detergent OTGP at a high concentration (9 mM), which provides a membrane-mimetic environment suitable for maintaining protein stability and solubility outside its membrane [28,40]. The use of other detergents such as Triton-114 or CHAPS resulted in loss of activity (data not shown).

After removal of proteins precipitating with 1.5 M $(NH_4)_2SO_4$, a gel filtration chromatography was used (Fig. S1) and LPH was purified with an 85-fold, a yield of 8.5% and a specific activity of 7.73×10^{-3}, as shown in Table S1.

The purified native LPH showed a molecular mass of 64,748 Da as determined by MALDI-TOF mass spectrometry (Fig. S2A) that is consistent with the calculated value based on the 569 amino acid sequence (GenBank code: CBY45494.1) reported previously by Yang et al. [12]. However, it was found that in solution, the protein existed as a homotrimer with a molecular mass of 215 kDa as observed by gel filtration chromatography (Fig. S2B). This result is different from that observed with linoleic acid hydratase from *L. acidophilus* (LAH) and from *Macrococcus caseolyticus* (MCH) which were found in solution as a homodimers [24,27].

3.2. Hydratase activity assay and identification of 10-HOE as the reaction product of LPH

The reaction of LPH with LA led to the formation of 10-hydroxy-12-*cis*-octadecenoic acid (10-HOE; 18:1 $^{\Delta 12Z}$) which according to GC, was the only reaction product (Fig. 2A) besides LA which was not fully converted. The mass spectrum of the isolated product (Fig. 2B and C) shows the characteristic peak at 169 m/z owing to fragmentation at the C12–13 double bond and peaks at 201 and 98 m/z, indicating cleavage of the hydroxyl group at the C10 position. These results, confirm the identity of the 10-HOE molecule as the reaction product.

3.3. FAD uptake

Hydratases that belong to the MCRA's family are known to be FAD-binding proteins, so this cofactor was added to LPH in increasing concentrations and it resulted in increasing hydratase activity as well until reaching a plateau at 55 μM where maximum activity (0.10 μmol 10-HOE/min/mg) is observed (Fig. 3). These findings are very similar with those obtained with *Macrococcus caseolitycus* hydratase [24]. According to Hill's equation fit, FAD binds to LPH in a cooperatively way (N = 2.3) and has a Kd value of 4.1 μM. The absence of FAD produces abolishment of enzymatic activity.

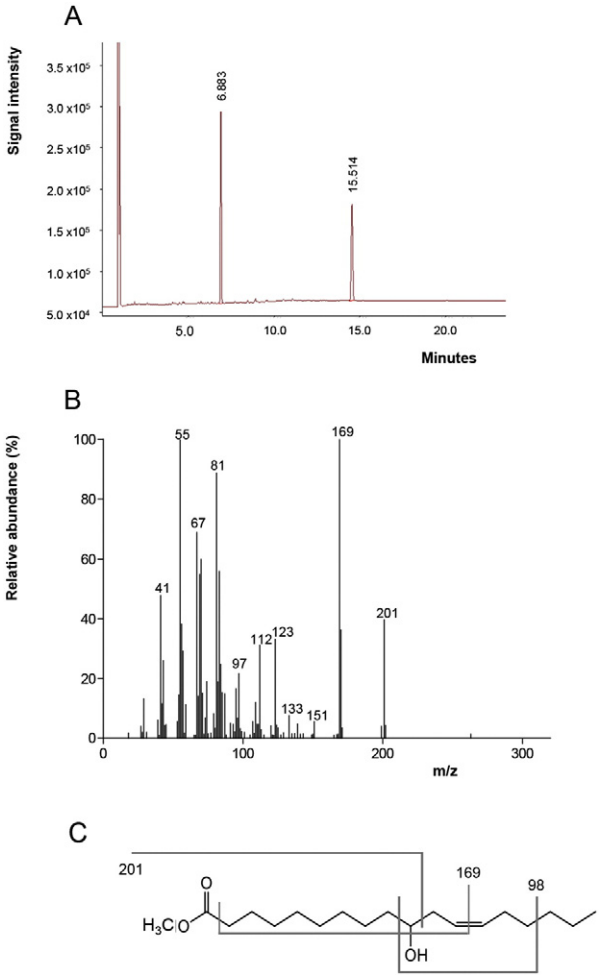

Fig. 2. Characterization of 10-HOE. (A) Total ion gas chromatogram of the conversion of LA (RT = 6.894 min) into 10-HOE (RT = 14.519 min). (B) Mass spectrum of 10-HOE after purification from the reaction mixture using RP-HPLC (Fig. S3) and (C) its fragmentation pattern.

3.4. Effect of reaction conditions on hydratase activity and stability

The variation of pH values on enzymatic activity of LPH reveals that optimal production of 10-HOE occurs at pH 6.5 and 7.0 (Fig. 4A). The pH was varied from 5.0 to 9.0 using 50 mM sodium acetate buffer (pH 5.0

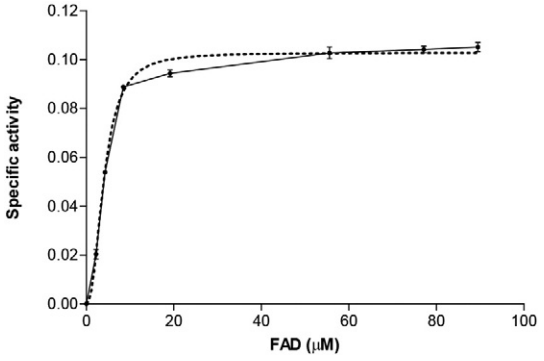

Fig. 3. Effect of FAD concentration in hydratase activity of LPH. The specific activity was calculated as μmol of 10-HOE/min/mg of protein (see Section 2.3).

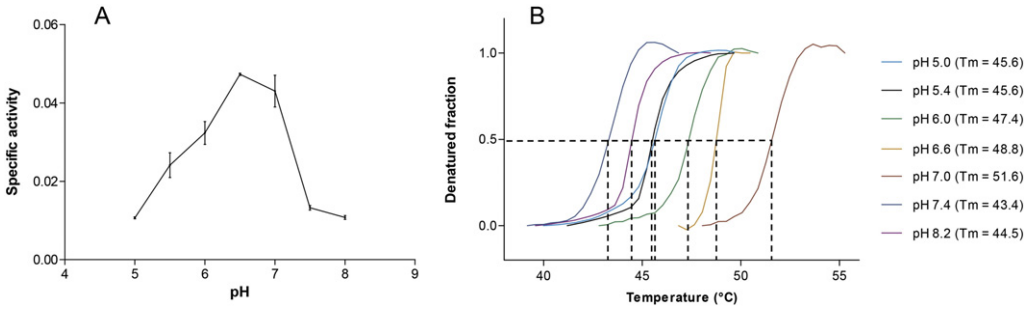

Fig. 4. Effect of pH on LPH. (A) Specific activity, calculated as μmol of 10-HOE/min/mg of protein (see Section 2.3). (B) Thermal stability at different pH values. The different melting point values (Tm) were calculated at the inflection point (dotted black lines) of the transition temperatures using Boltzmann's sigmoidal fit.

and 5.5), 50 mM bis-tris buffer (pH 6.0, 6.5 and 7.0) and 50 mM tris buffer (pH 7.5, 8.0).

Notably, the thermal stability of the protein is higher at pH 7.0 than at pH 6.4–6.6 (Fig. 4B) where the Tm value is increased from 48.7 °C to 51.6 °C at pH 7.0. Acid pH values, below pH 6.5, still allow the enzymatic activity with reduced yields but decrease the thermal stability of the protein whereas the lowest activity and stability of LPH was found in pH values above 7.0. The effect of pH value on thermal stability of LPH was not independent of the salt type used to buffer the different solutions since the protein showed a preference for sodium lactate and acetate salts in pH values below 7.0 and for glycine salt in pH above 8.0 (according to the composition of Wizard pH buffer kit with 96 different conditions).

In addition, $MgCl_2$, $(NH_4)_2SO_4$, dodecyl-β-maltoside, polyethylene glycol 400 and ethanol were the only additives, out of the 96 tested (see Section 2.7), that also increased the thermal stability of LPH (Fig. 5).

3.5. Structural modeling of LPH and its interaction with LA

A three-dimensional structure of LPH was calculated (Fig. 6A) (with a confidence of 0.8752) by homology modeling using an *ab initio* method based on the amino acid sequence of the protein (GenBank code: CBY45494.1) combined with the crystallographic structure of LAH (PDB code: 4ia5) due to their moderate sequence identity. Further analysis using DIAL server [41] resulted in the identification of 3 intricately connected domains: Domain 1 (colored in light blue in Fig. 6A) (residues 1–50, 229–352 and 482–549) has a mixed α/β fold composed of five parallel β-sheets between three helixes on the inner part and three antiparallel β-sheets on the outer part of the protein. This particular arrangement is denoted as Rossmann-like fold found in many FAD and NAD(P)-binding proteins which is also found on LAH, EMH (PDB code: 4uir) [42] and PAI (PDB code: 2bab) [21]. Domain 2 (colored in bubblegum pink in Fig. 6A) (residues 51–132, 209–228 and 353–481) has also a mixed α/β fold and consists of five antiparallel β-sheets surrounded closely by four helixes and furtherly by three more helixes that are in contact with the other two domains. Domain 3 (colored in wheat in Fig. 6A) (residues 133–208 and 550–569) is practically an all α fold and corresponds to the C-terminus of the protein.

Overall, LPH holds practically the same tertiary structure as LAH (Fig. 6B), with the exception of loops which showed high difference in terms of RMSD (Fig. S4) however, the biggest difference is that LAH holds two extra helixes that account for additional fourth domain.

Molecular docking assays resulted in the identification of two putative LA sites (Fig. 7): Site 1 was found to be a hydrophobic pocket located in domain 3 and the amino acid residues that have a direct interaction with LA are Leu149, Ile153, Met154, Pro156, Met206, Ile210 and Phe213 (Fig. 7C). Interestingly, the fatty acid molecule is arranged around Met154 which acts as a rigid pole for the hydrocarbon chain at the mid part whereas at the ω-end of LA, the molecule is packed between Leu149, Ile210, Phe213 and Leu560. Finally, the carboxylate of LA appears to be solvent-exposed as it was found on the outer surface of the protein and interacting with Pro156 through hydrophobic interaction (Fig. 7C) according to LigPlot analysis (Fig. S5A) [43].

An additional active site (site 2) was found at the core of the protein along with the putative FAD-binding site (Fig. 7B). Site 2 was found to be a hydrophobic cavity located at the interface of domains 1, 2 and 3. A schematic representation of the amino acid residues that are considered to have a direct interaction with LA are depicted in Fig. 7C. From there, it can be highlighted that the fatty acid molecule is also arranged around a methionine residue (Met81) acting as a rigid pole for the hydrocarbon chain at the mid part. All of the amino acid residues and the FAD molecule as well, are forming hydrophobic contacts with the ligand according to LigPlot analysis (Fig. S5B) [43].

Site 2 was found to be in contact with the putative FAD-binding site through hydrophobic contacts. A schematic representation of the amino acid residues interacting with the FAD molecule is depicted in Figure S5C. According to LigPlot analysis [43], FAD establishes hydrogen bonds with the main chain of residues Leu18, Ser19, Asn49, Arg80, Met81, Ser300, Glu513 and Thr524 whereas the rest of the residues interact through hydrophobic interactions.

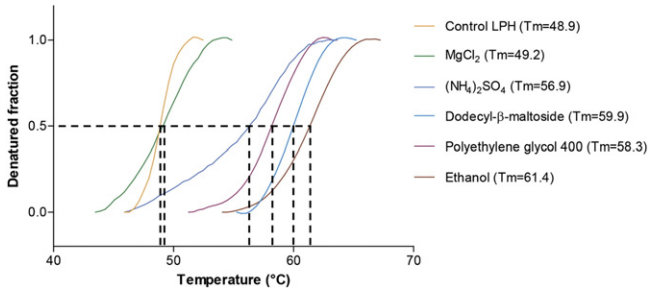

Fig. 5. Effect of additives on LPH thermal stability. The different melting point values (Tm) were calculated at the inflection point (dotted black lines) of the transition temperatures using Boltzmann's sigmoidal fit.

3.6. Analysis of the interaction of LPH with POPC:DMPC liposomes

Native LPH was reconstituted in POPC:DMPC proteoliposomes as stated before. The system was dual-labeled so that both, phospholipid bilayer and LPH were visualized simultaneously by confocal fluorescence microscopy (Fig. 8).

The results show that the Rhodamine B-labeled LPH is arranged around the surface of β-BODIPY® FL C_5-HPC-labeled liposomes. This interaction is clearly observed only on the surface of the lipid bilayer suggesting that LPH establishes a peripheral association with biomimetic membranes (Fig. 8, C2).

Control experiments of liposomes without the protein showed the absence of any association around the surface of the liposome (Fig. S6).

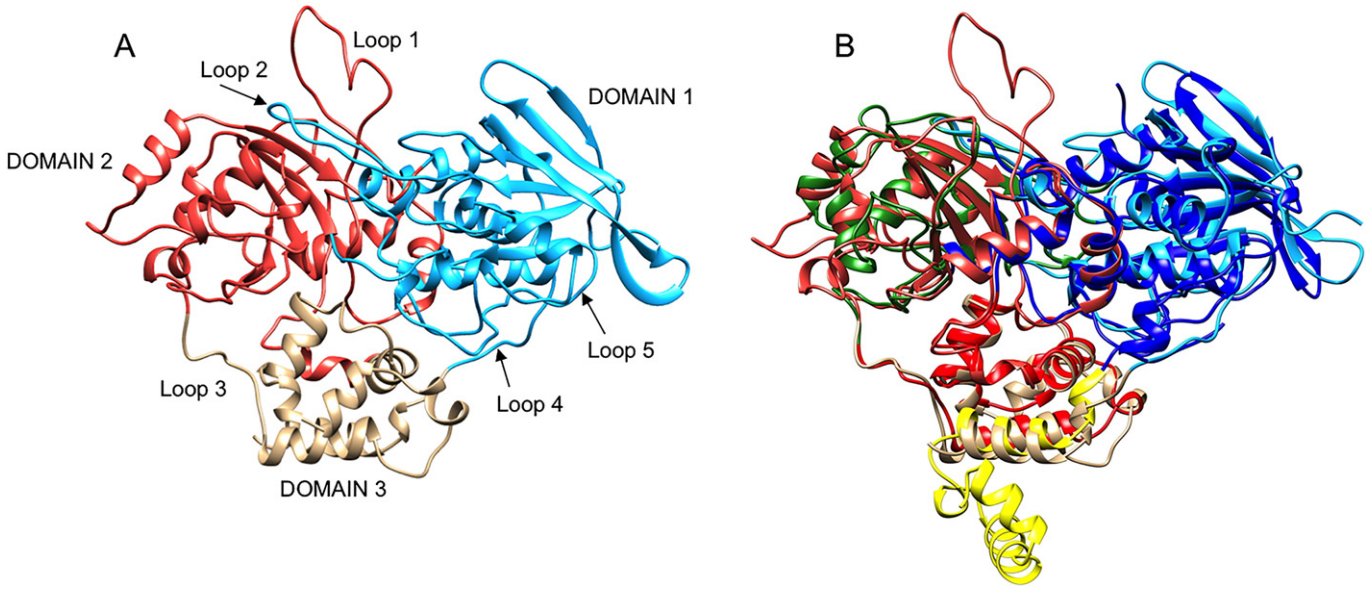

Fig. 6. Three-dimensional structure of LPH. (A) Depiction of domain 1 (light blue) which possess a Rossmann-like folding, domain 2 (bubblegum pink) that consist of α/β fold and domain 3 (wheat) which is all α-helix fold. Highly disordered regions were found as large loops: loop 1 (residues 42–78), loop 2 (residues 298–322), loop 3 (residues 119–141), loop 4 (residues 490–508) and loop 5 (541–552). (B) Structural comparison of LPH and LAH. Colors of LAH are the same as the original reference [27] (domain 1 in blue, domain 2 in green, domain 3 in red and domain 4 in yellow).

4. Discussion

Hydratase activity towards polyunsaturated fatty acids like linoleic and oleic acid poses a detoxification mechanism in bacteria since these lipids inhibit the development of plasmatic membranes and enoyl-ACP reductase activity [4,26]. MCRA protein family in a various intestinal bacteria has been found to possess this enzymatic activity in order to survive and adapt their growth in fatty acid-rich environments [7]. Hence, it is essential for cell defense in hostile environments. Additionally, the hydration of linoleic acid in lactic bacteria such as *L. plantarum*, has been proved to be the first step in the production of bioactive conjugated linoleic acid [6] which has many beneficial properties. In this study, 64.7 kDa linoleic acid hydratase from *L. plantarum* (LPH) was isolated in its native form from the plasmatic membrane fraction using OTGP as

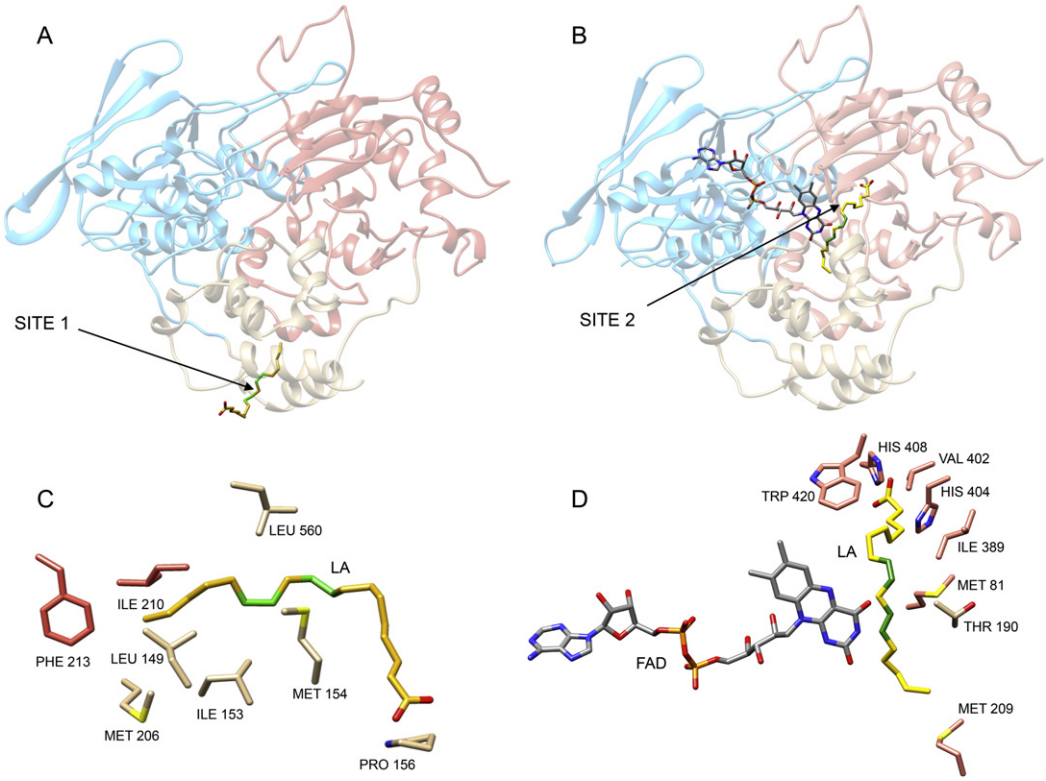

Fig. 7. Architecture of the binding sites of LPH with LA. (A) Overall location of LA in site 1 at the hydrophobic pocket in domain 3 and (B) in FAD-binding site 2 at the hydrophobic cavity between the three domains. (C) Depiction of residues that account for active site 1 and (D) for active site 2. LA molecule is colored in yellow whereas double bonds (carbons 9–10 and 12–13) are colored in green.

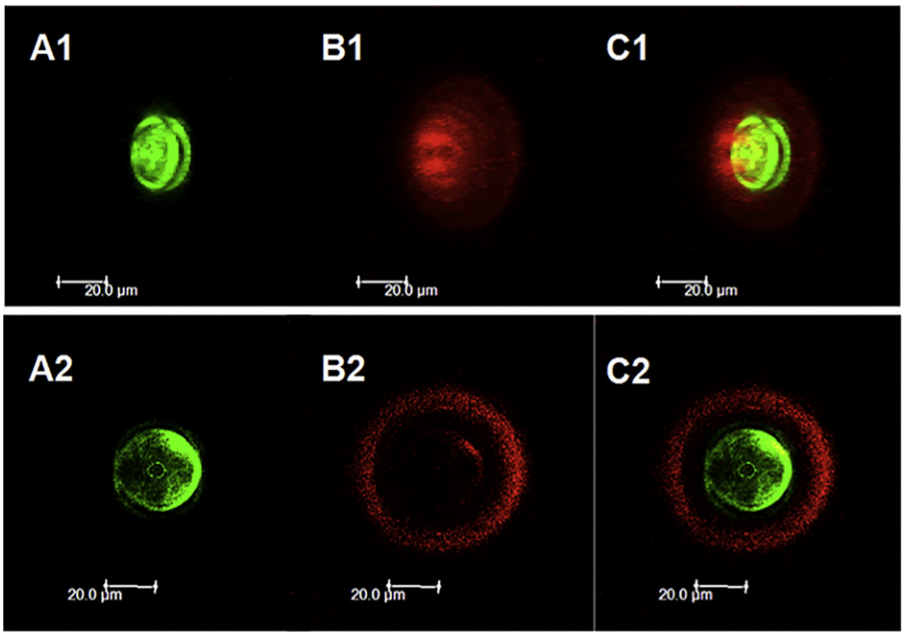

Fig. 8. CFM of LPH proteoliposomes. Assembly and association of the protein with biomimetic membranes. (A) Green fluorescence belongs to hydrophobic β-BODIPY® FL C_5-HPC signal. It shows the phospholipid bilayer shape and topology while (B) red fluorescence belongs to hydrophilic Rhodamine B signal bound to the protein. (C) Combined and color-merged images of both signals. Images in row 1 show a convex cross section of one proteoliposome whereas images in row 2 show a front view.

the disrupting detergent of the membranes. It was found that the protein undergoes oligomerization in solution resulting in the formation of an active homotrimer, in contrast with recombinant LAH and MCH which were characterized as homodimers [24,27]. Oligomerization might occur due to interaction between the highly disorder regions that can be found on each monomer such as large loops (Fig. 6A).

Biochemical characterization of the native protein showed that optimal stability occurs on an environment set at a pH between 6.5 and 7.0 and with the addition of either $MgCl_2$ (50 mM), $(NH_4)_2SO_4$ (500 mM), dodecyl-β-maltoside (2.5%), polyethylene glycol 400 (25%) or ethanol (15%). The maximum production of 10-HOE from LA occurs also between pH 6.5 and 7.0.

The amino acid sequence analysis of LPH using BLAST server and Clustal W server [44,45] (Fig. S7) showed a moderate identity with other fatty acid hydratases: 32% with LAH, 30% with BBH and MCH and 31% with SPH and EMH. Additionally, all these hydratases that also belong to the MCRA's family are known to be FAD-binding proteins. Experimentally it was demonstrated that LPH binds this cofactor cooperatively with a Kd value of 4.1 µM (Fig. 3). The FAD-binding domain of LPH has been previously defined as a 47 residue cluster (from Met6 to Gly52) [12]; however, from the sequence alignment analysis (Fig. S7), eighteen extra residues were added to this domain (65 amino acids in total) and from them, Gly15, Gly17, Gly52, Gly78, Gly79, Arg80, Met81, Thr297, Gly512, Phe523 and Thr524 are highly conserved among FAD-binding domain in hydratases. Additionally, the domain presents the characteristic $GxG(x)_9L(x)_{17-23}G$ motif consistent with FAD- and NAD(P)-binding Rossmann folds [46] and structurally, is located at the core of LPH, directly in contact with LA binding-site 2

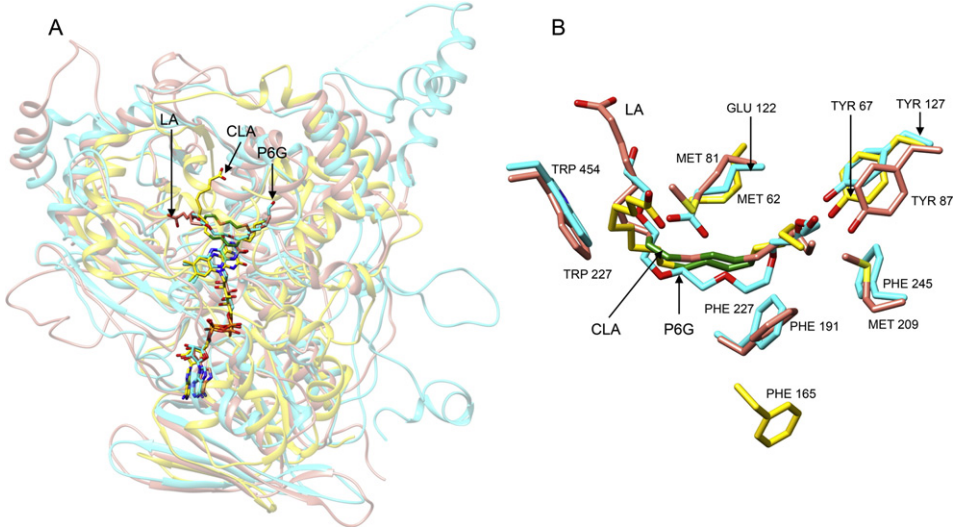

Fig. 9. Structural comparison of FAD-binding related proteins. LPH (depicted in pink), EMH (depicted in cyan) and PAI (depicted in yellow. (A) FAD molecules and active sites from each of the three proteins are located practically in identical regions at the core of the enzymes. (B) Identification of conserved amino acid residues involved in the active site. The molecule located in the active site of EMH was reported to be a 6 carbon–polyethylene glycol (P6G) [42], whereas the substrate of PAI was the bioactive isomer 10-*trans*-12-*cis*-CLA (CLA) [21]. Substrate of LPH was LA (LA).

(Fig.7B). The FAD molecule was found to hold practically the same location and conformation than that identified experimentally on FAD-binding EMH and PAI (Fig. 8A).

Hydration of LA catalyzed by LPH, produces a hydroxylated enoic acid (10-HOE). The homology model of the protein with the docked ligand molecule may be helpful to comprehend the binding mode: LA binds to site 1 located on a cavity on domain 3 (Fig. 7A) which resembles almost identically the external binding site of LAH [27]. The most important feature in this site is that, in both proteins, LA molecule arranges around a methionine residue (Met156 in LPH and Met154 in LAH) which acts as a rigid pole for the hydrocarbon chain (Fig. 7D). LA also binds to site 2 which is a hydrophobic pocket at the core of LPH very close to the isoalloxazine ring of FAD molecule. This site resembles very much the binding site of EMH [42] and PAI [21,22] (Fig. 9A) since some amino acid residues are in identical conformation (Fig. 9B). Surprisingly, in site 2, the hydrocarbon chain of LA also arranges around a methionine residue (Met81). This behavior is consistent with the binding mode of PAI [21] which also binds LA around a methionine residue (Met64). In both sites, the ligand anchors to the cavity by hydrophobic interactions throughout the hydrocarbon chain. These findings, might lead to the assumption that LA binds first to LPH through external site 1 and after that, the protein could undergo a conformational change mostly in one of the many loops that are found in the structure of LPH (Fig. 6A) and a channel might be formed, from the surface to the interior of the protein where the FAD molecule is lodged (Fig. 7). These results shed light into the binding mode and conserved residues of hydratases from the *Lactobacillus* genus involved in the conversion of LA as a detoxifying mechanism against polyunsaturated fatty acids.

Hydration, as well as isomerization activity of LA in *L. plantarum* have always been reported in the plasmatic membrane-associated fraction [9], however no further studies were carried out to confirm or characterize the nature of the membrane–protein interaction. In this study, we reconstituted LPH in POPC:DMPC fluorescent liposomes which mimicked the native membrane environment of the cell. It was demonstrated through confocal fluorescence microscopy analysis, that LPH is a peripheral membrane protein since it interacts with the lipid bilayer in a superficial or extrinsic way (Fig. 8). During the purification process, the use of $(NH_4)_2SO_4$ (1.5 M) as a chaotropic salt, may have allowed the extraction or detachment of LPH from the membranes while maintaining it in a soluble state (Table S1). In this work, we suggest that the superficial attachment of the hydratase could be mediated by electrostatic interactions between one of the positive-cationic patches on the surface of LPH (Fig. 10) and the phosphate-oxygen polar heads of phospholipids, since they have proven to have a very large negative surface potential available for electrostatic binding with various molecules [47].

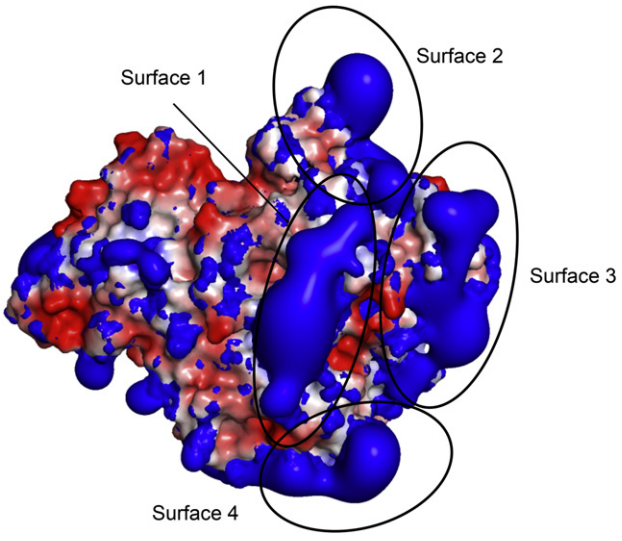

Fig. 10. Surface potential of LPH. Positive-cationic patches (in blue) of the protein were calculated using ABPS program [48]. Surfaces 1, 2 and 4 are the only sites available for electrostatic interaction with phosphate–oxygen from phospholipids while surface 3 is involved in the vicinity of active site.

Peripheral-electrostatic association of LPH with membranes through potential surfaces 1, 2 or 4 would allow the active site to bind extracellular fatty acid molecules and so, the peripheral nature of LPH can also be explained in terms of its enzymatic activity as the main goal of fatty acids hydratases is to participate in the cell detoxification from a fatty acid-rich environment, so in order to act as the first receptor, it needs to bind the toxic molecule and catalyze its hydration before it reaches plasmatic membranes and in this way, prevent the disruption of the lipid bilayers due to the kinked geometry of the unsaturated fatty acids [3] and also prevent the inhibition of enoyl-ACP reductase activity [4].

5. Conclusions

Hydratase from *L. plantarum*, here denoted as LPH, has enzymatic activity towards linoleic acid producing a hydroxylated enoic acid and was previously described only as a FAD-containing protein belonging to MCRA family. Here, we obtained the protein in its native form and explored, for the first time, two important attributes that were unknown: first, the location of the putative binding sites within the protein architecture and its characterization. Site 1 locks the hydrocarbon chain of the fatty acid through hydrophobic interactions but leaves the carboxylate group out of the cavity, facing the protein exterior and site 2 is located at the core of the protein in close contact with the FAD molecule suggesting a relocation of the substrate from the exterior to the interior where the enzymatic reaction takes place. Also, we identified a conserved methionine amino acid residue that plays an important role on packing the ligand on both binding sites. Second, we determined that interaction of native LPH with biomimetic membranes is peripheral and proposed that it is mediated by electrostatic interaction of one of the large positive surface potentials that can be found on the protein. The relevance of this study lies upon the fact that the peripheral location of membrane-associated LPH, has a functional implication on the cell detoxification from polyunsaturated fatty acids such as linoleic acid.

Acknowledgments

This work was financially supported by the Programa de Apoyos para Proyectos de Investigación e Innovación Tecnológica (PAPIIT) in Mexico (funds IN207013). A special thanks to Consejo Nacional de Ciencia y Tecnología (CONACyT) in Mexico for the student scholarship CVU/Reg: 271399/223477. The authors wish to thank Carmen Márquez, Lucero Ríos and F. Javier Pérez from Instituto de Química, UNAM for their technical support in the analysis of fatty acids and Carmen Santamaría for the experimental preparation of liposomes.

The confocal laser scanning microscopy study was done in the microscopy laboratory of CIIDIR-IPN, Unidad Sinaloa, Guasave, Sinaloa, Mexico.

Appendix A. Supplementary data

Supplementary data to this article can be found online at http://dx.doi.org/10.1016/j.bbamem.2015.09.014.

References

[1] D.L. Greenway, K.G. Dyke, Mechanism of the inhibitory action of linoleic acid on the growth of *Staphylococcus aureus*, J. Gen. Microbiol. 115 (1979) 233–245.
[2] M.K. Raychowdhury, R. Goswami, P. Chakrabarti, Effect of unsaturated fatty acids in growth inhibition of some penicillin-resistant and sensitive bacteria, J. Appl. Bacteriol. 59 (1985) 183–188.
[3] H. Keweloh, H.J. Heipieper, Trans unsaturated fatty acids in bacteria, Lipids 31 (1996) 129–137.

[4] C.J. Zheng, J.S. Yoo, T.G. Lee, H.Y. Cho, Y.H. Kim, W.G. Kim, Fatty acid synthesis is a target for antibacterial activity of unsaturated fatty acids, FEBS Lett. 579 (2005) 5157–5162.

[5] A. Buccioni, M. Decandia, S. Minieri, G. Molle, A. Cabiddu, Lipid metabolism in the rumen: new insights on lipolysis and biohydrogenation with an emphasis on the role of endogenous plant factors, Anim. Feed Sci. Technol. 174 (2012) 1–25.

[6] M.R. Maia, L.C. Chaudhary, L. Figueres, R.J. Wallace, Metabolism of polyunsaturated fatty acids and their toxicity to the microflora of the rumen, Antonie Van Leeuwenhoek 91 (2007) 303–314.

[7] N. McKain, K.J. Shingfield, R.J. Wallace, Metabolism of conjugated linoleic acids and 18: 1 fatty acids by ruminal bacteria: products and mechanisms, Microbiol-Sgm 156 (2010) 579–588.

[8] I.S. Nam, P.C. Garnsworthy, Biohydrogenation of linoleic acid by rumen fungi compared with rumen bacteria, J. Appl. Microbiol. 103 (2007) 551–556.

[9] S. Kishino, J. Ogawa, K. Yokozeki, S. Shimizu, Linoleic acid isomerase in Lactobacillus plantarum AKU1009a proved to be a multi-component enzyme system requiring oxidoreduction cofactors, Biosci. Biotechnol. Biochem. 75 (2011) 318–322.

[10] S. Kishino, S.B. Park, M. Takeuchi, K. Yokozeki, S. Shimizu, J. Ogawa, Novel multicomponent enzyme machinery in lactic acid bacteria catalyzing C=C double bond migration useful for conjugated fatty acid synthesis, Biochem. Biophys. Res. Commun. 416 (2011) 188–193.

[11] S. Kishino, M. Takeuchi, S.B. Park, A. Hirata, N. Kitamura, J. Kunisawa, H. Kiyono, R. Iwamoto, Y. Isobe, M. Arita, H. Arai, K. Ueda, J. Shima, S. Takahashi, K. Yokozeki, S. Shimizu, J. Ogawa, Polyunsaturated fatty acid saturation by gut lactic acid bacteria affecting host lipid composition, Proc. Natl. Acad. Sci. U. S. A. 110 (2013) 17808–17813.

[12] B. Yang, H. Chen, Y. Song, Y.Q. Chen, H. Zhang, W. Chen, Myosin-cross-reactive antigens from four different lactic acid bacteria are fatty acid hydratases, Biotechnol. Lett. 35 (2013) 75–81.

[13] B. Yang, H. Chen, Z. Gu, F. Tian, R.P. Ross, C. Stanton, Y.Q. Chen, W. Chen, H. Zhang, Synthesis of conjugated linoleic acid by the linoleate isomerase complex in food-derived lactobacilli, J. Appl. Microbiol. 117 (2014) 430–439.

[14] A. Bhattacharya, J. Banu, M. Rahman, J. Causey, G. Fernandes, Biological effects of conjugated linoleic acids in health and disease, J. Nutr. Biochem. 17 (2006) 789–810.

[15] I. Churruca, A. Fernandez-Quintela, M.P. Portillo, Conjugated linoleic acid isomers: differences in metabolism and biological effects, Biofactors 35 (2009) 105–111.

[16] N.M. Racine, A.C. Watras, A.L. Carrel, D.B. Allen, J.J. McVean, R.R. Clark, A.R. O'Brien, M. O'Shea, C.E. Scott, D.A. Schoeller, Effect of conjugated linoleic acid on body fat accretion in overweight or obese children, Am. J. Clin. Nutr. 91 (2010) 1157–1164.

[17] N.S. Kelley, N.E. Hubbard, K.L. Erickson, Conjugated linoleic acid isomers and cancer, Br. J. Nutr. 137 (2007) 2599–2607.

[18] S. Benjamin, F. Spener, Conjugated linoleic acids as functional food: an insight into their health benefits, Nutr. Metab. 6 (2009) 36.

[19] C.R. Kepler, S.B. Tove, Biohydrogenation of unsaturated fatty acids. 3. Purification and properties of a linoleate delta-12-cis, delta-11-trans-isomerase from Butyrivibrio fibrisolvens, J. Biol. Chem. 242 (1967) 5686–5692.

[20] S.S. Peng, M.D. Deng, A.D. Grund, R.A. Rosson, Purification and characterization of a membrane-bound linoleic acid isomerase from *Clostridium sporogenes*, Enzym. Microb. Technol. 40 (2007) 831–839.

[21] A. Liavonchanka, E. Hornung, I. Feussner, M.G. Rudolph, Structure and mechanism of the *Propionibacterium acnes* polyunsaturated fatty acid isomerase, Proc. Natl. Acad. Sci. U. S. A. 103 (2006) 2576–2581.

[22] A. Liavonchanka, M.G. Rudolph, K. Tittmann, M. Hamberg, I. Feussner, On the mechanism of a polyunsaturated fatty acid double bond isomerase from *Propionibacterium acnes*, J. Biol. Chem. 284 (2009) 8005–8012.

[23] L.E. Bevers, M.W. Pinkse, P.D. Verhaert, W.R. Hagen, Oleate hydratase catalyzes the hydration of a nonactivated carbon–carbon bond, J. Bacteriol. 191 (2009) 5010–5012.

[24] Y.C. Joo, K.W. Jeong, S.J. Yeom, Y.S. Kim, Y. Kim, D.K. Oh, Biochemical characterization and FAD-binding analysis of oleate hydratase from *Macrococcus caseolyticus*, Biochimie 94 (2012) 907–915.

[25] E. Rosberg-Cody, A. Liavonchanka, C. Gobel, R.P. Ross, O. O'Sullivan, G.F. Fitzgerald, I. Feussner, C. Stanton, Myosin-cross-reactive antigen (MCRA) protein from Bifidobacterium breve is a FAD-dependent fatty acid hydratase which has a function in stress protection, BMC Biochem. 12 (2011) 9.

[26] A. Volkov, A. Liavonchanka, O. Kamneva, T. Fiedler, C. Goebel, B. Kreikemeyer, I. Feussner, Myosin cross-reactive antigen of *Streptococcus pyogenes* M49 encodes a fatty acid double bond hydratase that plays a role in oleic acid detoxification and bacterial virulence, J. Biol. Chem. 285 (2010) 10353–10361.

[27] A. Volkov, S. Khoshnevis, P. Neumann, C. Herrfurth, D. Wohlwend, R. Ficner, I. Feussner, Crystal structure analysis of a fatty acid double-bond hydratase from *Lactobacillus acidophilus*, Acta crystallographica. Sect.D Biol. Crystallogr. 69 (2013) 648–657.

[28] M. le Maire, P. Champeil, J.V. Moller, Interaction of membrane proteins and lipids with solubilizing detergents, Biochim. Biophys. Acta 1508 (2000) 86–111.

[29] P. Luna, M. Juarez, M.A. de la Fuente, Gas chromatography and silver-ion high-performance liquid chromatography analysis of conjugated linoleic acid isomers in free fatty acid form using sulphuric acid in methanol as catalyst, J. Chromatogr. A 1204 (2008) 110–113.

[30] S. Boivin, S. Kozak, R. Meijers, Optimization of protein purification and characterization using Thermofluor screens, Protein Expr. Purif. 91 (2013) 192–206.

[31] S. Raman, R. Vernon, J. Thompson, M. Tyka, R. Sadreyev, J.M. Pei, D. Kim, E. Kellogg, F. DiMaio, O. Lange, L. Kinch, W. Sheffler, B.H. Kim, R. Das, N.V. Grishin, D. Baker, Structure prediction for CASP8 with all-atom refinement using Rosetta, Proteins 77 (2009) 89–99.

[32] Y.F. Song, F. DiMaio, R.Y.R. Wang, D. Kim, C. Miles, T.J. Brunette, J. Thompson, D. Baker, High-resolution comparative modeling with RosettaCM, Structure 21 (2013) 1735–1742.

[33] P. Emsley, B. Lohkamp, W.G. Scott, K. Cowtan, Features and development of Coot, Acta Crystallogr. D 66 (2010) 486–501.

[34] R.A. Laskowski, M.W. Macarthur, D.S. Moss, J.M. Thornton, Procheck — a program to check the stereochemical quality of protein structures, J. Appl. Crystallogr. 26 (1993) 283–291.

[35] K. Arnold, L. Bordoli, J. Kopp, T. Schwede, The Swiss-MODEL workspace: a web-based environment for protein structure homology modelling, Bioinformatics 22 (2006) 195–201.

[36] G.M. Morris, R. Huey, W. Lindstrom, M.F. Sanner, R.K. Belew, D.S. Goodsell, A.J. Olson, AutoDock4 and AutoDockTools4: automated docking with selective receptor flexibility, J. Comput. Chem. 30 (2009) 2785–2791.

[37] A.D. Bangham, M.M. Standish, J.C. Watkins, Diffusion of univalent ions across lamellae of swollen phospholipids, J Mol Biol 13 (1965) 238-&.

[38] J.L. Rigaud, D. Levy, Reconstitution of membrane proteins into liposomes, Methods Enzymol. 372 (2003) 65–86.

[39] S. Bibi, R. Kaur, M. Henriksen-Lacey, S.E. McNeil, J. Wilkhu, E. Lattmann, D. Christensen, A.R. Mohammed, Y. Perrie, Microscopy imaging of liposomes: from coverslips to environmental SEM, Int. J. Pharm. 417 (2011) 138–150.

[40] D.V. Tulumello, C.M. Deber, Efficiency of detergents at maintaining membrane protein structures in their biologically relevant forms, Biochim. Biophys. Acta 1818 (2012) 1351–1358.

[41] G. Pugalenthi, G. Archunan, R. Sowdhamini, DIAL: a web-based server for the automatic identification of structural domains in proteins, Nucleic Acids Res. 33 (2005) W130–W132.

[42] M. Engleder, T. Pavkov-Keller, A. Emmerstorfer, A. Hromic, S. Schrempf, G. Steinkellner, T. Wriessnegger, E. Leitner, G.A. Strohmeier, I. Kaluzna, D. Mink, M. Schurmann, S. Wallner, P. Macheroux, K. Gruber, H. Pichler, Structure-based mechanism of oleate hydratase from *Elizabethkingia meningoseptica*, Chembiochem: a European, J. Chem. Biol. 16 (2015) 1730–1734.

[43] A.C. Wallace, R.A. Laskowski, J.M. Thornton, Ligplot – a program to generate schematic diagrams of protein ligand interactions, Protein Eng. 8 (1995) 127–134.

[44] S.F. Altschul, W. Gish, W. Miller, E.W. Myers, D.J. Lipman, Basic local alignment search tool, J. Mol. Biol. 215 (1990) 403–410.

[45] M.A. Larkin, G. Blackshields, N.P. Brown, R. Chenna, P.A. McGettigan, H. McWilliam, F. Valentin, I.M. Wallace, A. Wilm, R. Lopez, J.D. Thompson, T.J. Gibson, D.G. Higgins, Clustal W and clustal X version 2.0, Bioinformatics 23 (2007) 2947–2948.

[46] G. Kleiger, D. Eisenberg, GXXXG and GXXXA motifs stabilize FAD and NAD(P)-binding Rossmann folds through C-alpha-H···O hydrogen bonds and van der Waals interactions, J. Mol. Biol. 323 (2002) 69–76.

[47] A. Mashaghi, P. Partovi-Azar, T. Jadidi, N. Nafari, P. Maass, M.R.R. Tabar, M. Bonn, H.J. Bakker, Hydration strongly affects the molecular and electronic structure of membrane phospholipids, J Chem Phys 136 (2012).

[48] N.A. Baker, D. Sept, S. Joseph, M.J. Holst, J.A. McCammon, Electrostatics of nanosystems: application to microtubules and the ribosome, Proc. Natl. Acad. Sci. U. S. A. 98 (2001) 10037–10041.